PROCEEDINGS OF SCIENCE

Phase structure of three and four flavor QCD *

Christian A. Welzbacher†
Institut fuer Theoretische Physik, Justus-Liebig-Universitaet Giessen, Heinrich-Buff-Ring 16, D-35392 Giessen, Germany
E-mail: Christian.A.Welzbacher@physik.uni-giessen.de

Christian S. Fischer
Institut fuer Theoretische Physik, Justus-Liebig-Universitaet Giessen, Heinrich-Buff-Ring 16, D-35392 Giessen, Germany
E-mail: Christian.Fischer@theo.physik.uni-giessen.de

Jan Luecker
Institut fuer Theoretische Physik, Universitaet Heidelberg, Philosophenweg 16, D-69120 Heidelberg, Germany
Institut fuer Theoretische Physik, Goethe-Universitaet Frankfurt, Max-von-Laue-Strasse 1, D-60438 Frankfurt/Main, Germany
E-mail: Jan.Luecker@theo.physik.uni-giessen.de

Recent results for the phase structure of QCD at finite temperature and light-quark chemical potential are summarized, where the cases of $N_f = 2+1$ and $N_f = 2+1+1$ dynamical quark flavors are considered. From solutions of a coupled set of truncated Dyson-Schwinger equations for the quark and gluon propagators of Landau gauge QCD the order parameters for the chiral and deconfinement transitions are obtained. Based on very good agreement with results from lattice QCD for zero chemical potential the phase diagram, featuring a putative critical end-point at large chemical potential, is studied.

Keywords: Critical end point, QCD phase diagram, Dyson-Schwinger equations

9th International Workshop on Critical Point and Onset of Deconfinement - CPOD2014, 17-21 November 2014
ZiF (Center of Interdisciplinary Research), University of Bielefeld, Germany

*A talk with similar content was given by Christian A. Welzbacher at the FAIRNESS2014 (22nd to 27th of September 2014, Vietri sul Mare, Italy).

†Speaker.

PoS(CPOD2014)074

1. Introduction

In recent years, the interest of experimental and theoretical studies in heavy ion collisions and particularly the phase diagram of QCD grew rapidly. In facilities such as RHIC at BNL, ALICE at LHC and CBM at the future FAIR facility experimentalists (will) search for possible signals of phase transitions and a putative critical end point (*CEP*). On the theoretical side, calculations of the discretized QCD on the lattice has established a crossover transition at small chemical potential, see e.g. [1, 2] for $N_f = 2+1$ flavors. In our work we approach the QCD phase diagram with the functional method of Dyson-Schwinger equations and put particular emphasis on the possible influence of the charm quark on the phase structure of QCD [3]. One expects the contribution of the charm quark to the equation of state starts to become significant around top LHC energies. However, possibly even at smaller temperatures close or above the light-quark crossover region, effects of charm quarks, although predicted to be small by perturbation theory [4], may not be entirely negligible. Within lattice QCD preliminary results on calculations with $N_f = 2+1+1$ flavors for transition temperatures and the equation of state using staggered [5, 6] and Wilson type quarks [7] are available. Here we summarize recent results for the phase diagram at zero and finite chemical potential within the non-perturbative framework of Dyson-Schwinger equations. At zero chemical potential we compare with results from lattice QCD for the quark condensate and the unquenched gluon propagator before we discuss our results for the phase diagram and the critical end point for $N_f = 2+1$ and $N_f = 2+1+1$ quark flavors.

2. Framework

Dyson-Schwinger equations (*DSEs*) are the equations of motion for the n-point functions of QCD. In Fig. 1 we show the DSE for the quark propagator. This quark 2-point function is the foundation of an infinite tower of coupled integral equations, which are in principle ab initio if solved completely and self-consistently. Therefore the quark propagator would already hold all the (exact) informations about the phase diagram of QCD. In practice, however, in most cases one needs to impose a truncation using input from other sources such as symmetries, constraints or other methods like lattice QCD.

The truncation used in this work has been developed over the past few years (see [8, 9, 10, 11, 3]) and consists of two key points. The first part of the truncation is depicted in Fig. 2, showing the approximation in the DSE for the Landau gauge gluon propagator. In order to calculate this quantity we use input from lattice QCD for the quenched gluon propagator (denoted by the yellow dot), replacing diagrams with internal gluons and Faddeev-Popov ghosts. To this quantity we add a quark loop for each flavor. In this simplification of the gluon DSE we neglect all the second order unquenching effects in the Yang-Mills diagrams, but it is ensured that we take the important temperature effects of the quenched gluon propagator into account. Additionally the unquenched gluon propagator inherits a dependence on the temperature and the chemical potential via the quark loops, giving a contribution to the thermal mass, which agrees well with predictions from hard-thermal-loop perturbation theory for high temperatures. The gluon propagators at finite temperature

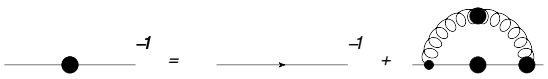

Figure 1: The quark Dyson-Schwinger equation.

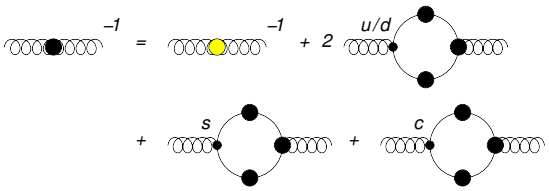

Figure 2: The truncated gluon Dyson-Schwinger equation.

T and quark-chemical potential μ is given by

$$D_{\alpha\beta}(p) = P^L_{\alpha\beta}(p)\frac{Z^L(p)}{p^2} + P^T_{\alpha\beta}(p)\frac{Z^T(p)}{p^2}\,, \tag{2.1}$$

with momentum $p = (\omega_n, \vec{p})$, $\omega_n = 2n\pi T$ for bosons. The projectors $P^{L,T}_{\alpha\beta}$ are longitudinal (L) and transverse (T) with respect to the heat bath and given by

$$P^T_{\alpha\beta} = (1-\delta_{\alpha 4})\,(1-\delta_{\beta 4})\left(\delta_{\alpha\beta} - \frac{p_\alpha p_\beta}{\vec{p}^{\,2}}\right), \tag{2.2}$$

$$P^L_{\alpha\beta} = P_{\alpha\beta} - P^T_{\alpha\beta}\,, \tag{2.3}$$

where $P_{\alpha\beta}$ is the transverse projector with respect to the four momentum.

The second element of our truncation is an approximation for the full quark-gluon vertex. Information on this vertex can be gathered from lattice QCD or from solutions of its DSE. Corresponding studies at zero temperature and chemical potential are in progress, for recent works see e.g. [13, 14] in the DSE framework and [15, 16] in the functional renormalization group approach. At finite temperature, however, information from these sources is not yet available. We therefore use a functional form for this vertex which combines information from the well-known perturbative behavior at large momenta and an approximate form of the Slavnov-Taylor identity at small momenta studied long ago by Ball and Chiu [17]. The explicit form of this approximate expression for the quark-gluon vertex is discussed in Refs. [9, 10, 3] and shall not be repeated here for brevity. It contains one open parameter, called d_1 in the following, which controls the infrared strength of the vertex and sets the temperature scale for in-medium calculations. Furthermore, via the Ball-Chiu construction, it contains dressing functions of the two attached quarks. Therefore our ansatz for the quark-gluon vertex is flavor, as well as temperature and chemical potential dependent. The construction of the quark-gluon vertex additionally ensures to keep the multiplicative renormalizability of our equations.

To investigate the influence of the charm quark, we developed two approaches to set the IR-strength of the quark-gluon vertex as well as the physical masses of the quarks. The first one (called Sets A_{Nf}) connects our calculations to lattice QCD, since the IR-strength and light-quark mass is fixed to reproduce the (pseudo-) critical temperature $T_C \approx 155$ MeV from [1] for N_f=2+1 flavors at zero chemical potential. Since in a crossover region there are different definitions of a critical temperature, we point out that the chosen one is defined via the inflection point of the chiral condensate to match the definition used in [1]. The mass of the strange quark is chosen to be 27 times the light-quark mass. To this setup we merely added a charm quark with a mass of 300 MeV at a

renormalization point of 80 GeV, without adjusting the IR-strength. In our second approach (called Sets B_{Nf}) we set the IR-strength in the quark-gluon vertex and the physical quark masses self-consistently by fixing the pion decay constant, as well as the pion, kaon and η_C mass in the very same truncation via the Bethe-Salpether equation, separately for N_f=2+1 and N_f=2+1+1. This was possible due to recent progress in the Bethe-Salpether framework [12]. To describe the (pseudo-) critical temperature of our system, we calculate the chiral condensate

$$\langle\bar{\psi}\psi\rangle^f = Z_2^f Z_m^f N_c T \sum_n \int \frac{d^3p}{(2\pi)^3} \mathrm{Tr}_D \left[S^f(p)\right], \tag{2.4}$$

where $S^f(p)$ is the calculated quark propagator for flavor f, Z_2^f and Z_m^f are the corresponding wave-function and quark mass renormalization constants, respectively, and $N_c = 3$ is the number of colors. Due to the behavior of the quark massfunction in the ultraviolet, any quark flavor with non-zero bare quark mass leads to a condensate which is quadratically divergent and needs to be regularized. In order to cancel this divergence one defines the regularized chiral condensate

$$\Delta_{l,s} = \langle\bar{\psi}\psi\rangle_l - \frac{m_l}{m_s}\langle\bar{\psi}\psi\rangle_s . \tag{2.5}$$

The quantity $\Delta_{l,s}(T)/\Delta_{l,s}(T=0)$ can therefore be considered as an order parameter for the chiral transition. In our work we extract T_C either by considering the maximum of the derivative of this quantity with respect to temperature (*inflection point*) or with respect to the mass of the light quarks (*chiral susceptibility*).

3. Results

In this section we show the results calculated within the framework discussed in the previous section. In Fig. 3 we compare the electric (longitudinal) part of the gluon propagator for N_f=2 and a pion mass of 316 MeV with lattice data from [18]. The parameter d_1 and the physical quark mass are fixed in the manner of Set B. Note that our result, determined first in [10], has been a prediction, verified later by the lattice results. Therefore the quite good agreement for the unquenched gluon, featuring an inversion of the temperature ordering when going from the quenched to the unquenched case, serves as a further justification for our truncation scheme. In Fig. 4 the same quantity is shown, in this case for Set A_{2+1}. We observe the same inversion of the temperature ordering as well as the suppression of the maximum after the unquenching. In Fig. 5 we show the regularized chiral condensate at μ=0 MeV for all sets of interest, compared to lattice data taken from [1]. We observe a very good agreement of Set A_{2+1} (dashed red line) with the lattice data, not only in the scale (T_C, controlled by the choice of d_1 as shown in Fig. 6) but also in the steepness of the regularized condensate, which is a non-trivial result. Additionally we find that by merely adding the charm quark in Set A (dash-dotted blue line), the curve is shifted towards lower temperatures. This is an effect caused by adding the charm quark to the system without adjusting the physical scale (d_1). To investigate the physical content of this behavior, we consider the Sets B (solid black line), where we find that by self-consistently readjusting the scale, the charm quark has no visible effect.

Fig. 7 shows the phase diagrams for Sets B. It immediately becomes apparent, that the negligible

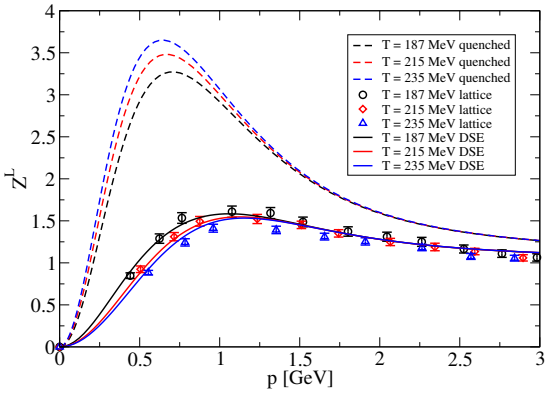

Figure 3: Electric part of the gluon dressing functions for N_f=2, m_π=316 MeV.

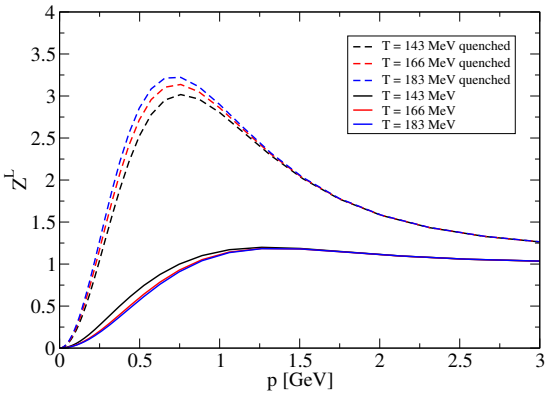

Figure 4: Electric part of the gluon dressing functions for Set A_{2+1}.

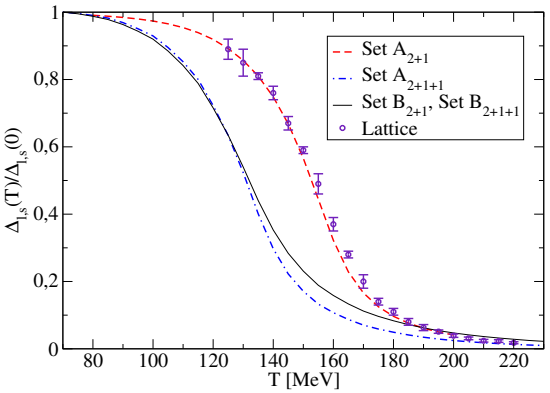

Figure 5: $\Delta_{l,s}$ at μ=0 MeV [3].

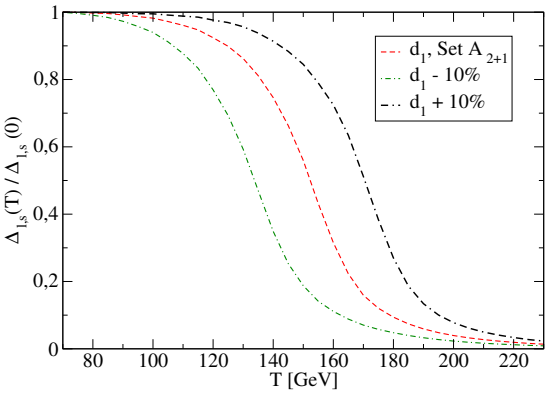

Figure 6: Influence of d_1 on $\Delta_{l,s}$.

contribution of the charm quark which we observed for μ=0 MeV in Fig. 5, continues to be small for the whole T-μ-plane for both, chiral and deconfinement transition. The deconfinement transition was fixed via the Polyakov loop of the minimum of the background field potential (see [11] for more details), where the inflection point is used. On the other hand, the critical temperature in the chiral crossover region was defined by the maximum of the chiral susceptibility. This partly explains the gap for small chemical potential between the crossover lines. The results in Fig. 7 suggest that there is almost no influence of the charm quark on the transition temperatures, provided the internal scales are controlled by external input. For the prediction of the QCD phase diagram shown in Fig. 8 we therefore return to lattice input (Set A_{2+1}). In this plot, the critical temperature for the crossover region is in both cases, chiral and deconfinement transition, defined by the inflection point method. One can see, that the chiral crossover (dashed black line) becomes ever steeper with increasing chemical potential and turns into a critical end point (CEP) at

$$(T^c, \mu_q^c) = (115, 168)\,\mathrm{MeV}. \tag{3.1}$$

To guide the eye we added lines for μ_B/T=2 and μ_B/T=3 as well as predictions for the curvature of the chiral transition line from lattice extrapolations for $N_f = 2+1$ of different groups at imaginary and zero chemical potential into the real chemical potential region [19, 20, 21]. The agreement

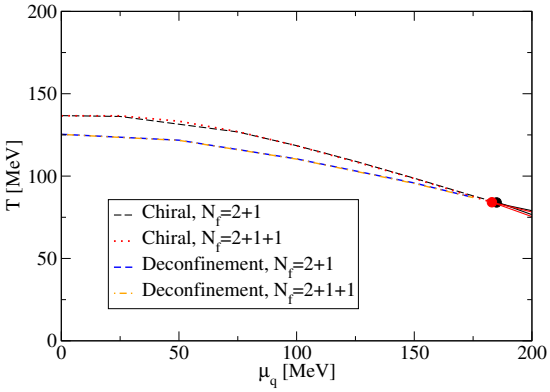

Figure 7: Phase diagram Sets B [3].

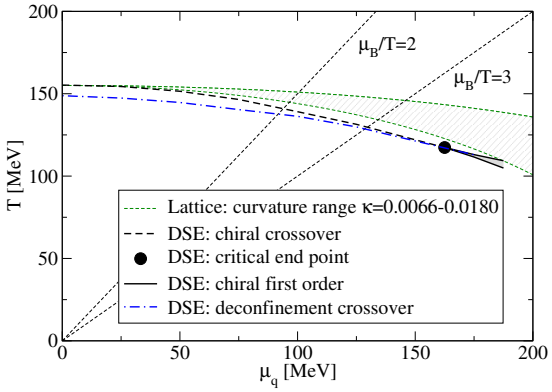

Figure 8: Phase diagram Set A_{2+1} [3].

between the lattice extrapolation and our DSE results is quite satisfactory. We close with the remark that potential effects of baryons onto the location of the critical endpoint have not yet been taken into account, neither in the lattice extrapolations of the curvature, nor in our DSE approach. In order to turn this qualitative study into a quantitative one, these effects need to be addressed. Thus the close agreement of both approaches, although interesting, may very well not be the final word.

Acknowledgements

This work has been supported by the Helmholtz Alliance HA216/EMMI and by ERC-AdG-290623 as well as the Helmholtz International Center for FAIR within the LOEWE program of the State of Hesse. Christian A. Welzbacher gratefully recieved support from EMMI (ExtreMe Matter Institute of the Helmholtz Association).

References

[1] S. Borsanyi *et al.*, *JHEP* **1009** (2010) 073 [arXiv:1005.3508 [hep-lat]].

[2] A. Bazavov, T. Bhattacharya, M. Cheng, C. DeTar, H. T. Ding, S. Gottlieb, R. Gupta and P. Hegde *et al.*, *Phys. Rev. D* **85** (2012) 054503 [arXiv:1111.1710 [hep-lat]].

[3] C. S. Fischer, J. Luecker and C. A. Welzbacher, *Phys. Rev. D* **90**, no. 3, 034022 (2014) [arXiv:1405.4762 [hep-ph]].

[4] M. Laine and Y. Schroder, *Phys. Rev. D* **73** (2006) 085009 [arXiv:0603048 [hep-ph]].

[5] A. Bazavov *et al. PoS LATTICE* **2013** (2014) 154 [arXiv:1312.5011 [hep-lat]].

[6] S. Borsanyi, G. Endrodi, Z. Fodor, A. Jakovac, S. D. Katz, S. Krieg, C. Ratti and K. K. Szabo, *JHEP* **1011** (2010) 077 [arXiv:1007.2580 [hep-lat]].

[7] F. Burger, G. Hotzel, M. Mueller-Preussker, E. M. Ilgenfritz and M. P. Lombardo, [arXiv:1311.1631 [hep-lat]].

[8] C. S. Fischer, *Phys. Rev. Lett.* **103** (2009) 052003 [arXiv:0904.2700 [hep-ph]].

[9] C. S. Fischer, A. Maas and J. A. Muller, *Eur. Phys. J. C* **68** (2010) 165 [arXiv:1003.1960 [hep-ph]].

[10] C. S. Fischer and J. Luecker, *Phys. Lett. B* **718** (2013) 1036 [arXiv:1206.5191 [hep-ph]].

[11] C. S. Fischer, L. Fister, J. Luecker and J. M. Pawlowski, *Phys. Lett. B* **732** (2014) 273 [arXiv:1306.6022 [hep-ph]].

[12] W. Heupel, T. Goecke and C. S. Fischer, *Eur. Phys. J. A* **50** (2014) 85 [arXiv:1402.5042 [hep-ph]].

[13] R. Williams, [arXiv:1404.2545 [hep-ph]].

[14] A. C. Aguilar, D. Binosi, D. Ibañez and J. Papavassiliou, *Phys. Rev. D* **90** (2014) 6, 065027 [arXiv:1405.3506 [hep-ph]].

[15] M. Mitter, J. M. Pawlowski and N. Strodthoff, [arXiv:1411.7978 [hep-ph]].

[16] J. Braun, L. Fister, J. M. Pawlowski and F. Rennecke, [arXiv:1412.1045 [hep-ph]].

[17] J. S. Ball and T.-W. Chiu *Phys. Rev. D* **22** (1980) 2542.

[18] R. Aouane, F. Burger, E.-M. Ilgenfritz, M. Müller-Preussker and A. Sternbeck, *Phys. Rev. D* **87** (2013) 11, 114502 [arXiv:1212.1102 [hep-lat]].

[19] G. Endrodi, Z. Fodor, S. D. Katz and K. K. Szabo, *JHEP* **1104** (2011) 001 [arXiv:1102.1356 [hep-lat]].

[20] O. Kaczmarek, F. Karsch, E. Laermann, C. Miao, S. Mukherjee, P. Petreczky, C. Schmidt and W. Soeldner *et al.*, *Phys. Rev. D* **83** (2011) 014504 [arXiv:1011.3130 [hep-lat]].

[21] P. Cea, L. Cosmai and A. Papa, *Phys. Rev. D* **89** (2014) 7, 074512 [arXiv:1403.0821 [hep-lat]].